



Turun yliopisto
University of Turku

GENESIS AND EVOLUTION OF BRITTLE STRUCTURES IN SOUTHWESTERN FINLAND AND WESTERN SOUTH AFRICA

Insights into Fault Reactivation, Fluid Flow and
Structural Maturity in Precambrian Cratons

Jussi Mattila

University of Turku

Faculty of Mathematics and Natural Sciences

Department of Geography and Geology

Geology and Mineralogy

Supervised by

Dr. Timo Kilpeläinen
Department of Geography and Geology
University of Turku, Finland

Dr. Peter Sorjonen-Ward
Geological Survey of Finland
Kuopio, Finland

Reviewed by

Prof. Mikael Rinne
Department of Civil and
Environmental Engineering
Aalto University, Espoo, Finland

Dr. Kerstin Saalman
Geological Survey of Norway
Trondheim, Norway

Opponent

Prof. Paul Bons
Department of Geosciences
University of Tübingen
Tübingen, Germany

The originality of this thesis has been checked in accordance with the University of Turku quality assurance system using the Turnitin OriginalityCheck service.

ISBN 978-951-29-6050-7 (PRINT)

ISBN 978-951-29-6051-4 (PDF)

ISSN 0082-6979

Multiprint Oy - Turku, Finland 2015

Abstract

The bedrock of old crystalline cratons is characteristically saturated with brittle structures formed during successive superimposed episodes of deformation and under varying stress regimes. As a result, the crust effectively deforms through the reactivation of pre-existing structures rather than by through the activation, or generation, of new ones, and is said to be in a state of 'structural maturity'. By combining data from Olkiluoto Island, southwestern Finland, which has been investigated as the potential site of a deep geological repository for high-level nuclear waste, with observations from southern Sweden, it can be concluded that the southern part of the Svecofennian shield had already attained structural maturity during the Mesoproterozoic era. This indicates that the phase of activation of the crust, i.e. the time interval during which new fractures were generated, was brief in comparison to the subsequent reactivation phase. Structural maturity of the bedrock was also attained relatively rapidly in Namaqualand, western South Africa, after the formation of first brittle structures during Neoproterozoic time. Subsequent brittle deformation in Namaqualand was controlled by the reactivation of pre-existing strike-slip faults. In such settings, seismic events are likely to occur through reactivation of pre-existing zones that are favourably oriented with respect to prevailing stresses. In Namaqualand, this is shown for present day seismicity by slip tendency analysis, and at Olkiluoto, for a Neoproterozoic earthquake reactivating a Mesoproterozoic fault.

By combining detailed field observations with the results of paleostress inversions and relative and absolute time constraints, seven distinct superimposed paleostress regimes have been recognized in the Olkiluoto region. From oldest to youngest these are: (1) NW-SE to NNW-SSE transpression, which prevailed soon after 1.75 Ga, when the crust had sufficiently cooled down to allow brittle deformation to occur. During this phase conjugate NNW-SSE and NE-SW striking strike-slip faults were active simultaneous with reactivation of SE-dipping low-angle shear zones and foliation planes. This was followed by (2) N-S to NE-SW transpression, which caused partial reactivation of structures formed in the first event; (3) NW-SE extension during the Gothian orogeny and at the time of rapakivi magmatism and intrusion of diabase dikes; (4) NE-SW transtension that occurred between 1.60 and 1.30 Ga and which also formed the NW-SE-trending Satakunta graben located some 20 km north of Olkiluoto. Greisen-type veins also formed during this phase. (5) NE-SW compression that postdates both the formation of the 1.56 Ga rapakivi granites and 1.27 Ga olivine diabases of the region; (6) E-W transpression during the early stages of the Mesoproterozoic Sveconorwegian orogeny and which also predated (7) almost coaxial E-W extension attributed to the collapse of the Sveconorwegian orogeny.

The kinematic analysis of fracture systems in crystalline bedrock also provides a robust framework for evaluating fluid-rock interaction in the brittle regime; this is essential in assessment of bedrock integrity for numerous geo-engineering applications, including groundwater management, transient or permanent CO₂ storage and site investigations for permanent waste disposal. Investigations at Olkiluoto revealed that fluid flow along fractures is coupled with low normal tractions due to in-situ stresses and thus deviates from the generally accepted critically stressed fracture concept, where fluid flow is concentrated on fractures on the verge of failure. The difference is linked to the shallow conditions of Olkiluoto - due to the low differential stresses inherent at shallow depths, fracture activation and fluid flow is controlled by dilation due to low normal tractions. At deeper settings, however, fluid flow is controlled by fracture criticality caused by large differential stress, which drives shear deformation instead of dilation.

Keywords: brittle deformation, structural geology, structural maturity, fluid flow, seismicity, fault zones, paleostress analysis, slip tendency, dilation tendency, Olkiluoto, Namaqualand, Finland, South Africa

Tiivistelmä

Ajan saatossa erilaisten deformaatiovaiheiden ja jännityskenttien vaikutuksesta vanhat kiteiset peruskallion alueet saturoituvat hauraiden rakenteiden osalta. Saturoitumisen jälkeen kallioperä deformatuu pääasiallisesti vanhojen rakenteiden uudelleenaktivoitumisen kautta sen sijaan, että kallioperään syntyisi uusia hauraita rakenteita. Tätä saturoitunutta tilannetta kuvataan termillä 'rakenteellinen kypsyys'. Olkiluoto sijaitsee Lounais-Suomessa ja on ehdolla mahdolliseksi korkea-aktiivisen ydinjätteen loppusijoituspaikaksi. Vertaamalla Olkiluodosta ja Etelä-Ruotsista kerättyä aineistoa voitiin todeta, että eteläinen Svekofenninen kuori saturoitui hauraiden rakenteiden suhteen ja saavutti siten rakenteellisen kypsyyden jo Mesoproterotsooisien maailmankauden aikana. Tämän perusteella vaihe, jolloin uusia hauraita rakenteita muodostui, oli suhteellisen lyhyt verrattuna vaiheeseen, jonka aikana kallioperän deformaatio on tapahtunut olemassa olevien rakenteiden uudelleenaktivoitumisen kautta. Samanlainen kallioperän kehityskulku on havaittavissa myös Namaquamaan alueella Etelä-Afrikassa, jossa ensimmäiset hauraat rakenteet muodostuivat Neoproterotsooisella maailmankaudella. Tämän jälkeen hauras deformaatio tapahtui olemassa olevien strike-slip -tyyppisten siirrostojen uudelleenaktivoitumisen kautta. Näissä olosuhteissa on odotettavaa, että mahdollinen seismisyys keskittyy vanhoihin rakenteisiin, jotka ovat otollisessa asennossa vallitsevaan jännityskenttään nähden. Namaquamaan osalta seismisyyden osoitetaan keskittyvän slip tendency -analyysin avulla tunnistettuihin siirroksiin ja Olkiluodossa puolestaan Mesoproterotsooiseen siirrokseen, joka aktivoitui maanjäristyksessä Neoproterotsooisella maailmankaudella.

Yhdistämällä rakennusgeologiset havainnot, paleojännitysanalyysin tulokset sekä suhteelliset että absoluuttiset ikämääritykset oli Olkiluodon alueelta mahdollista määrittää seitsemän erilaista paleojännityskenttää: (1) NW-SE - NNW-SSE -suuntainen transpressio, joka vaikutti pian 1.75 Ga jälkeen kun kallioperä jäähtyi tasolle jossa hauraiden rakenteiden muodostuminen oli mahdollista. Tämän vaiheen aikana muodostui NNW-SSE- ja NE-SW-suuntaisia strike-slip-sirroksia ja kaakkoon loivasti kaatuvat hiertovyöhykkeet ja liuskeisuustasot uudelleenaktivoituivat synkinemaattisesti. Tätä vaihetta seurasi (2) N-S - NE-SW -suuntainen transpressio, joka aiheutti ensimmäisen vaiheen aikana muodostuneiden rakenteiden osittaista uudelleenaktivoitumista; (3) NW-SE -suuntainen ekstensio Gothian-orogeenin sekä rapakivigraniittien ja diabaasijuonien muodostumisen aikana; (4) NE-SW -suuntainen transtensio, joka vaikutti aikavälillä 1.60 - 1.30 Ga ja jonka seurauksena muodostui NW-SE-suuntainen Satakunnan graben-rakenne, joka sijaitsee n. 20 km Olkiluodosta pohjoiseen. Tämän vaiheen aikana muodostuivat myös Olkiluodon alueen greisen-juonet. (5) NE-SW kompressio, joka on iältään nuorempi kuin alueen 1.56 Ga-ikäiset rapakivigraniitit ja 1.27 Ga-ikäiset oliviinidiabaasit; (6) E-W-suuntainen transpressio Mesoproterotsooisien Svekonorjalaisen orogeenin alkuvaiheessa ja joka myös edelsi lähes koaksiaalista (7) E-W -suuntaista ekstensiota Svekonorjalaisen orogeenin loppuvaiheen romahduksen aikana.

Kiteisten kivien rakosysteemien kinemaattinen analyysi antaa myös viitekehykset fluidien ja kivimassan vuorovaikutusten tarkastelemiseen hauraissa olosuhteissa. Tämänkaltaisen tarkastelu on oleellista monissa rakennusgeologian sovelluksissa, kuten pohjavesien liikkeiden mallinnuksessa, CO₂:n väliaikaisessa ja pitkäkestoisessa varastoinnissa sekä jätteen pysyvän loppusijoituksen paikatutkimuksissa. Fluidien virtausta Olkiluodon kallioperän raoissa kontrolloi nykyisen jännitystilan aiheuttama alhainen normaalijännitys sopivan suuntaisissa raoissa. Tämä hydromekaaninen kytkentä poikkeaa yleisesti hyväksytyistä käsityksistä, jonka mukaan fluidit virtaavat kallioperän niissä raoissa, jotka ovat ns. kriittisessä jännitystilassa. Ero johtuu Olkiluodon rakojen sijainnista kallioperän pintaosassa, jossa alhaisten differentiaalijännitysten vuoksi raot aktivoituvat mekaanisesti alhaisten normaalijännitysten ja dilataation kautta. Kallioperän syvemmissä osissa fluidien virtausta raoissa määrittää suurempi differentiaalijännitys, jonka seurauksena raoissa tapahtuu dilataation sijaan siirrostumista.

Asiasanat: hauras deformaatio, rakennegeologia, rakenteellinen kypsyys, pohjaveden virtaus, seismisyys, siirrosvyöhyke, paleojännitysanalyysi, siirrostumispotentiaali, dilataatiopotentiaali, Olkiluoto, Namaquamaa, Suomi, Etelä-Afrikka

Contents

List of original publications	1
1 Introduction	2
2 Theory	4
2.1 The concept of stress	4
2.2 Slip and dilation tendency analysis	8
2.3 Paleostress analysis	12
2.3.1 Graphical stress inversion methods	13
2.3.2 Direct inversion methods	16
3 Review of the original publications	19
4 Discussion	22
4.1 Crustal evolution of southwestern Finland	22
4.2 Structural maturity	24
4.3 Fluid flow along fractures	25
4.4 Implications for seismicity	27
5 Conclusions	29
Acknowledgements	31
References	32

List of original publications

This thesis comprises of an introductory part (synopsis), followed by four peer-reviewed publications. Reference to the publications in the text is made with Roman numbers, as designated below.

Paper I: Mattila, J., Viola, G., 2014. New constraints on 1.7 Gyr of brittle tectonic evolution in southwestern Finland derived from a structural study at the site of a potential nuclear waste repository (Olkiluoto Island). *Journal of Structural Geology*, Volume 67, Part A, 50-74

Paper II: Viola, G., Zwingmann, H., Mattila, J., Käpyaho, A., 2013. K-Ar illite age constraints on the Proterozoic formation and reactivation history of a brittle fault in Fennoscandia. *Terra Nova*, Volume 25, Issue 3, 236–244

Paper III: Mattila, J., Tammisto, E., 2012. Stress-controlled fluid flow in fractures at the site of a potential nuclear waste repository, Finland. *Geology*, Volume 40, 299-302

Paper IV: Viola, G., Kounov, A., Andreoli, M.A.G., Mattila, J., 2012. Brittle tectonic evolution along the western margin of South Africa: More than 500 Myr of continued reactivation. *Tectonophysics*, Volumes 514–517, 93–114

J. Mattila's main contribution to the papers was as follows:

Paper I: Structural mapping and collection of fault-slip data from outcrops (together with G. Viola) and the underground facilities; processing, analysis and interpretation of the fault-slip data (together with G. Viola), analysis and discussion of the stress ratio variability; preparation of figures; writing most parts of the manuscript.

Paper II: Collection of clay samples (together with G. Viola and A. Käpyaho), interpretation of the K-Ar-results (together with G. Viola and A. Käpyaho); image-based grain-size analysis of the gouge samples; preparation of maps and some of the figures; writing parts of the manuscript.

Paper III. Processing and analysis of the fracture and stress data; preparation of the maps and figures; writing of the manuscript.

Paper IV. Processing of the present-day stress data and slip-tendency analysis; preparation of figures associated with the slip-tendency analysis; writing parts of the manuscript (associated with the slip tendency analysis).

1 Introduction

The understanding of past and present stresses acting on rock masses is a vital part of modern structural geology and plays an essential role in many geological applications such as civil engineering, mining, hydrocarbon exploration and extraction and, not least, in the deep geological disposal of high-level nuclear waste. Present day rock stresses affect, for example, the stability of underground excavations, the stability of faults, which is in turn linked to the seismological behaviour of the crust, and the permeability of rock matrix through the coupled hydro-mechanical behaviour of fractures. Past (paleo-) stresses are, on the other hand, pivotal to the general understanding of the conditions that led to the formation of existing structural networks and to past fluid flow pathways, which is an important parameter for the understanding the formation of hydrothermal ore deposits. In addition, knowledge of past stresses may yield insights into strain localisation mechanisms and structural activation processes within the crust and thus provide constraints on the potential future seismic behaviour of a site.

Unravelling the past deformation history in old crystalline terrains is difficult due to the typically protracted and complex evolution of the bedrock. It has been shown, however, that such complex histories can be investigated and unravelled (e.g. Saintot et al. 2011, Viola et al. 2009, Munier & Talbot 1993) and that the conditions leading to the formation of brittle structures and their subsequent reactivation with respect to time can be assessed.

This thesis and its accompanying papers investigate the brittle deformation histories of Olkiluoto, southwestern Finland (Figure 1A), and Namaqualand, western South Africa (Figure 1B). Olkiluoto has been evaluated as the potential site for a deep repository for spent high-level nuclear fuel whereas Vaalputs in Namaqualand hosts the site licensed for the disposal of low and intermediate-level nuclear waste. In order to derive a brittle deformation scheme for the two sites, structural observations from outcrops, drill cores and tunnels and satellite images are combined in order to characterise and understand the geometrical and kinematic attributes of respective brittle structures. The paleostress states of the two sites were analysed by the inversion of fault-slip data and by constraining the inversion procedure with the observations made in the field. The results are then combined into a conceptual brittle deformation scheme, further constrained with relative and absolute time criteria. In addition to the brittle deformation schemes of the two sites, the hydromechanical coupling of transmissive fractures and in-situ stresses at Olkiluoto are analysed and discussed with respect to the generally accepted coupling relations for fluid flow along fractures and in situ stresses.

The results from these studies are discussed in this thesis from the perspective of structural maturity, a newly coined term but a concept developed by Munier & Talbot (1993) to describe a condition whereby the crust becomes saturated of brittle structures, causing the bedrock to accommodate stresses through reactivation of existing structures rather than by the generation of new ones. The implications of structural maturity for fluid flow and potential seismicity are further discussed as the condition effectively dictates how old crust with a protracted evolutionary history behaves mechanically in response to current and also future stress regimes.

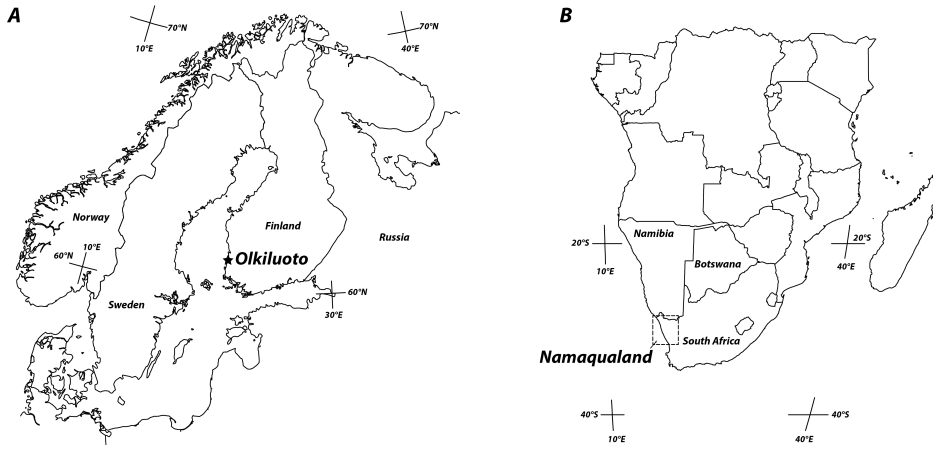


Figure 1: Location of the study areas: A. Olkiluoto in southwestern Finland and, B. Namaqualand in western South Africa.¹

¹All Figures have been made by the Author

2 Theory

2.1 The concept of stress

Stresses in rock are caused by the forces exerted on a rock volume. The two primary sources for these stresses are gravitational and tectonic forces, with the former (acting in a vertical sense) arising due to the weight of the overlying rock and the latter (acting with an essentially subhorizontal orientation) by the movements of the tectonic plates. In order to understand stresses mathematically, one needs to understand first the concept of a traction vector $\mathbf{t}(\mathbf{n})$ at a point, which is defined as the intensity of a force vector $\mathbf{f}(\mathbf{n})$ resolved on surface $A(\mathbf{n})$ (Figure 2), as the area A approaches zero:

$$\mathbf{t}(\mathbf{n}) = \lim_{A(\mathbf{n}) \rightarrow 0} \frac{\delta \mathbf{f}(\mathbf{n})}{\delta A(\mathbf{n})} \quad (1)$$

Here \mathbf{n} is the normal vector of the surface considered. The unit of the traction vector is $Nm^{-2} = \text{Pascal}$.

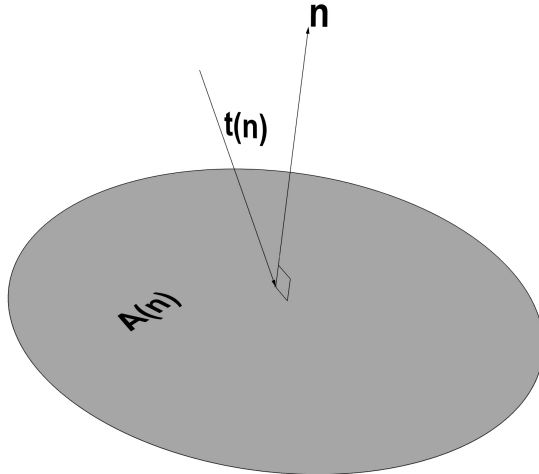


Figure 2: Traction vector $\mathbf{t}(\mathbf{n})$ on an infinitesimal surface $A(\mathbf{n})$ defined by its normal vector \mathbf{n} and located at a point.

The traction vector is dependent on the orientation of the surface upon which it acts. Therefore, in order to define the *stress* at a point, one needs to find a mathematical operator that can be used to compute the traction vector on any surface, defined by its normal \mathbf{n} , through the point in question. This operator is called the *stress tensor* $\boldsymbol{\sigma}$ and is defined as the matrix of the components of the traction vectors of three infinitesimal orthogonal surfaces located at a point:

$$\boldsymbol{\sigma} = \begin{bmatrix} \sigma_{xx} & \sigma_{xy} & \sigma_{xz} \\ \sigma_{yx} & \sigma_{yy} & \sigma_{yz} \\ \sigma_{zx} & \sigma_{zy} & \sigma_{zz} \end{bmatrix} \quad (2)$$

Given that, within a specific rock volume, the traction vectors on three orthogonal planes are known, the stress tensor can then be fully defined. In the stress tensor, the first row corresponds to the components of the traction vector acting on the plane perpendicular to the x-coordinate axis, the second row to the components of the traction vector acting on the plane perpendicular to y-coordinate axis and the third row, correspondingly, to the components of the traction vector acting on the plane perpendicular to z-coordinate axis (Figure 3). The first subscript of the traction vectors refer to the normal direction of the plane along which the traction vector is acting, while the second subscript distinguishes the different components of the traction vector, i.e. to which coordinate direction the component is oriented parallel to. For example, σ_{xx} refers to the traction vector component that acts on a surface with the normal in the x-direction, and in the direction of x, whereas σ_{xy} refers to the component which acts on a surface with the normal in the x-direction, and in the direction of the y-axis. Traction vector components, which are perpendicular to the surface the traction vector acts upon, are known as *normal traction* components, and components tangential to the surface, as *shear traction* components.

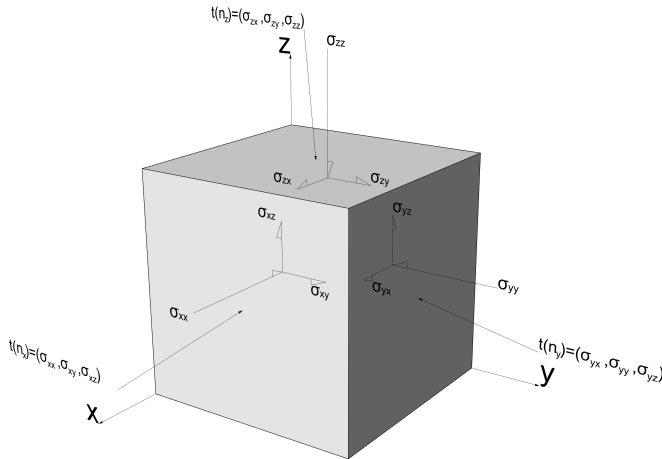


Figure 3: Stress elements on an infinitesimal cubic volume element.

When in equilibrium, the resultant moments on the sides of the cubic volume need to be zero, which means that the following relations between the shear traction components must hold:

$$\sigma_{xy} = \sigma_{yx} \quad \sigma_{yz} = \sigma_{zy} \quad \sigma_{zx} = \sigma_{xz} \quad (3)$$

and thus the stress tensor may be reduced to a simplified symmetric form with only six independent stress components:

$$\boldsymbol{\sigma} = \begin{bmatrix} \sigma_{xx} & \sigma_{xy} & \sigma_{xz} \\ \sigma_{xy} & \sigma_{yy} & \sigma_{yz} \\ \sigma_{xz} & \sigma_{yz} & \sigma_{zz} \end{bmatrix} \quad (4)$$

With a proper choice of coordinate axes, it is always possible to find a system wherein the traction vectors are perpendicular to the sides of the infinitesimal cube (Figure 3) and the shear tractions vanish. These axes define a so-called principal coordinate system and the resultant normal tractions represent the so-called principal stress vectors. Within the principal coordinate system, the stress tensor reduces into the form:

$$\boldsymbol{\sigma} = \begin{bmatrix} \sigma_1 & 0 & 0 \\ 0 & \sigma_2 & 0 \\ 0 & 0 & \sigma_3 \end{bmatrix} \quad (5)$$

where $(\sigma_1, 0, 0)$, $(0, \sigma_2, 0)$ and $(0, 0, \sigma_3)$ are the principal stress vectors and σ_1 , σ_2 and σ_3 further define the magnitudes of the maximum, intermediate and minimum principal stress, respectively. Mathematically, the principal stresses can be derived from the stress tensor by computing the eigenvalues of the tensor. The corresponding eigenvectors define the orientations of the principal stress vectors, that is, the orientation of the principal coordinate axes. The relative magnitudes of the principal stresses can be expressed through the stress ratio R :

$$R = \frac{(\sigma_2 - \sigma_3)}{(\sigma_1 - \sigma_3)} \quad (6)$$

The traction vector on any surface, as defined by its normal vector \mathbf{n} , can be computed by Cauchy's formula:

$$\mathbf{t}(\mathbf{n}) = \boldsymbol{\sigma} \mathbf{n} \quad (7)$$

which can be expressed in matrix representation as:

$$\begin{bmatrix} t_x \\ t_y \\ t_z \end{bmatrix} = \begin{bmatrix} \sigma_{xx} & \sigma_{xy} & \sigma_{xz} \\ \sigma_{xy} & \sigma_{yy} & \sigma_{yz} \\ \sigma_{xz} & \sigma_{yz} & \sigma_{zz} \end{bmatrix} \begin{bmatrix} n_x \\ n_y \\ n_z \end{bmatrix} \quad (8)$$

A traction vector on a surface can be decomposed into a component normal to the surface, called the *normal traction vector* (\mathbf{t}_n) and a component parallel to the surface, called the *shear traction vector* (\mathbf{t}_s) (Figure 3). These vectors can be computed for any

surface with a normal vector \mathbf{n} by solving the following equations:

$$\mathbf{t}_n = \mathbf{t}(\mathbf{n}) - \mathbf{t}_s = \mathbf{n}(\mathbf{t}(\mathbf{n}) \cdot \mathbf{n}) \quad (9)$$

$$\mathbf{t}_s = \mathbf{t}(\mathbf{n}) - \mathbf{t}_n = \mathbf{n} \times (\mathbf{t}(\mathbf{n}) \times \mathbf{n}) \quad (10)$$

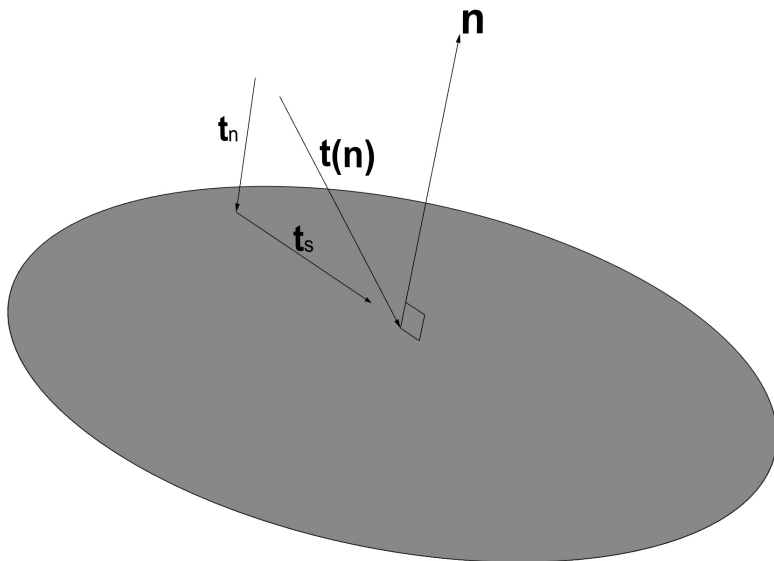


Figure 4: Normal (\mathbf{t}_n) and shear (\mathbf{t}_s) traction on a surface defined by its normal vector \mathbf{n} .

Equation (9) first computes the magnitude of the projection of the traction vector $\mathbf{t}(\mathbf{n})$ on the normal vector \mathbf{n} by the dot product $\mathbf{t}(\mathbf{n}) \cdot \mathbf{n}$, which then, through the product with the unit vector \mathbf{n} becomes equivalent to the normal traction vector \mathbf{t}_n . The shear traction vector \mathbf{t}_s can be computed either by the difference between the traction vector and the normal traction vector if the latter is known, or, as indicated by the right-hand side of equation (10), by first computing the cross product of the traction vector $\mathbf{t}(\mathbf{n})$ and the normal vector \mathbf{n} , which is equivalent to the $\mathbf{t}(\mathbf{n}) \times \mathbf{n}$ part of equation (10) - this product is a vector perpendicular to a plane defined by the traction and normal vectors and the resultant vector also defines the orientation for which the shear traction on the surface has a magnitude of 0. The second part of the right-hand side of the equation (10) computes the cross product of the normal vector \mathbf{n} and the vector $\mathbf{t}(\mathbf{n}) \times \mathbf{n}$, which is a vector located in the plane defined by the traction and normal vectors and is, in addition, perpendicular to the normal vector \mathbf{n} . The resultant vector is thus equal in

magnitude and orientation to the shear traction vector \mathbf{t}_s . The different components of the equation (10) are shown in Figure 5.

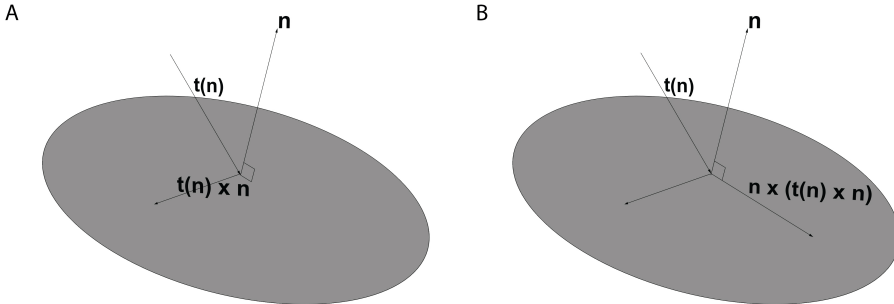


Figure 5: Computation of shear traction vector \mathbf{t}_s on a plane defined by the normal vector \mathbf{n} . A. Cross product between $\mathbf{t}(\mathbf{n})$ and \mathbf{n} results in the vector $\mathbf{t}(\mathbf{n}) \times \mathbf{n}$, which is in the direction of zero shear traction and perpendicular to the plane defined by $\mathbf{t}(\mathbf{n})$ and \mathbf{n} . B. Shear traction vector is computed with the cross product of \mathbf{n} and the vector $\mathbf{t}(\mathbf{n}) \times \mathbf{n}$.

2.2 Slip and dilation tendency analysis

When studying the mechanical behaviour of natural rock masses, we are commonly interested in non-equilibrium situations where we wish to describe and predict stresses and potential displacements on specific fracture surfaces and fracture networks. According to the Coulomb failure criterion, slip or reactivation on a fracture (simplified here as a planar surface with a normal \mathbf{n}) takes place if the magnitude of the shear traction on the fracture is equal to or exceeds the frictional resistance, which is proportional to the magnitude of the normal traction multiplied by the friction coefficient μ (e.g. Jaeger et al., 2007):

$$t_s \geq \mu t_n \quad (11)$$

or when

$$\frac{t_s}{t_n} \geq \mu \quad (12)$$

The ratio given in Equation (12) is known as the slip tendency T_s (Morris et al. 1996) and can be used as a proxy for the frictional failure of a fracture: when the value of the slip tendency is equal to or exceeds the friction coefficient, slip occurs and the fracture can be considered as critically stressed. Slip tendency values can be normalized by choosing a value for the friction coefficient considered to represent the failure condition in a given setting. Typically, values between $\mu = 0.6 - 0.9$ can be considered typical for frictional reactivation in a wide variety of settings (Byerlee 1978). For critically stressed fractures, the normalised slip tendency values are thus equal to or greater than unity.

The distribution of the normalised slip tendency values can be visualised with "normal versus shear traction" diagrams and by using Mohr circles to depict the stress state, as shown in Figure 6. In the chosen example, the $\sigma_1 - \sigma_3$ -circle is set to be tangential to the failure curve, thus describing a critical stress state where the maximum normalised slip tendency values are equal to one. These values are only found on faults whose poles are located exactly on the failure curve. Values above unity can only be found on faults located above the failure curve, but in the given stress state such faults cannot exist, as the $\sigma_1 - \sigma_3$ -circle does not cross the failure curve. Faults that are located below the failure curve have slip tendency values between 0 and 1. Constant shear to normal traction ratios form linear trends starting from the origin and the slope of these linear trends thus corresponds to constant slip tendency values. Values of 0 are attained on a line parallel to the x-axis, that is, when the shear traction has a value of 0.

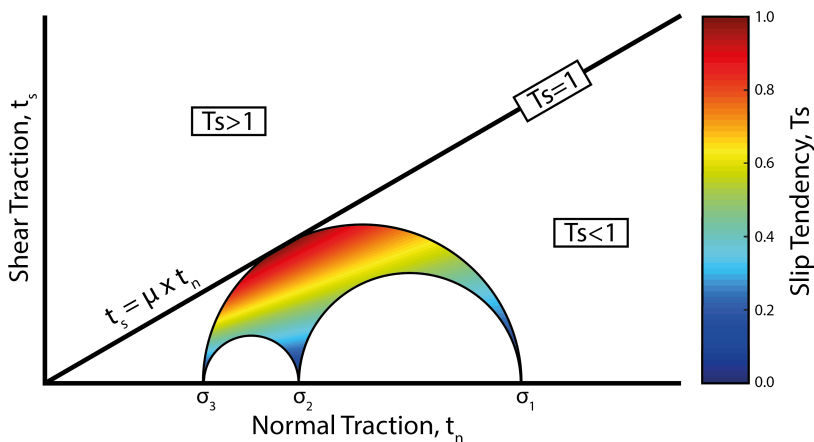


Figure 6: Normalised slip tendency values shown on a Mohr circle diagram for a stress state with a stress ratio ($R = (\sigma_2 - \sigma_3)/(\sigma_1 - \sigma_3)$) of 0.3. Faults that are located above the Coulomb failure curve have normalized slip tendency values greater than 1 and faults located below the curve have values less than 1. Faults that are located exactly on the failure curve have a value of 1.²

The slip tendency value and thus the reactivation potential of a fracture is dependent on the relative magnitudes of the principal stresses (Lisle & Srivastava 2004). To highlight this effect, slip tendency values for different fracture orientations and stress ratios are shown in an equal-area pole plot in Figure 7 for synthetic thrust-faulting (TF), strike-slip (SS) and normal-faulting (NF) stress regimes. In the Figure, each pole corresponds to a fracture with specific orientation and the colour of the pole is defined

²The Figure has been made by the Author using MatlabTM

by the normalised slip tendency value the fracture has in the given stress state. The slip tendency values are computed by assuming that the Mohr circles are tangential to the Coulomb failure curve and by normalising the results with the friction coefficient. As shown by the Figure, in the case of axial stresses, that is when the stress ratio is close to either 0 or 1 ($\sigma_3 = \sigma_2$ or $\sigma_2 = \sigma_1$, respectively), the poles to fractures with the highest slip tendency values form girdle-pattern around the σ_1 - and σ_3 -orientations, respectively. For stress ratio values close to 0, the poles to the fractures with the highest slip tendencies form a girdle-pattern around σ_1 , whereas for high values, the girdle is located around σ_3 . Typical bimodal conjugate-type reactivation patterns occur only when the stress ratios are close to 0.5. The differences in the slip-tendency patterns demonstrate the importance of the intermediate principal stress axis in the reactivation potential of fractures. Furthermore, they illustrate the fact that at very low and high stress ratios, the number of fracture orientations susceptible to reactivation is greater than for intermediate stress ratios (see also Morris & Ferrill 2009), and that the orientations of potentially critical fractures are much more diverse than could be expected for example from the simplistic Anderson's theory of faulting (Anderson 1905). When the effect of the intermediate stress axis is taken into consideration, it is seen that fractures which could be thought as having a non-optimal orientation with respect to the maximum and minimum stress axes may actually prove to be critically stressed.

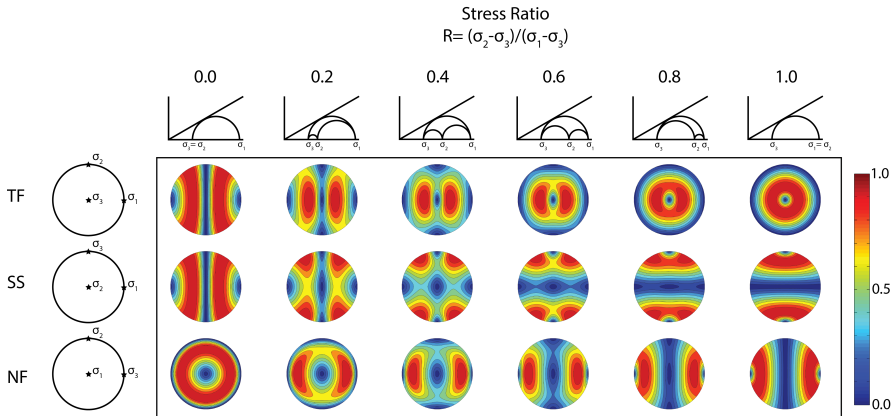


Figure 7: Slip tendency (T_s) values computed³ for all possible orientations in thrust-fault (TF), strike-slip (SS) and normal-fault (NF) regimes with varying stress ratios R . Slip tendency values are computed by assuming that the mohr arbelos are tangential to the Mohr-Coulomb failure curve and normalized with the friction coefficient. A value of 1.0 indicates thus the maximum possible slip tendency value in the given stress state and value 0 the minimum. Equal area, lower hemisphere projections.

If the effect of shear on an undulating fracture surface is neglected, the dilation of a fracture is mainly controlled by the normal traction such that the lower the normal

³Computations have been carried out by the Author using Matlab™

traction, the higher the dilation potential. In order to compare the dilation potential of fractures in different stress states, Ferrill et al. (1999) defined a normalized parameter called dilation tendency (T_d), which is computed through the following equation:

$$T_d = \frac{\sigma_1 - t_n}{\sigma_1 - \sigma_3} \quad (13)$$

The numerator in Equation (13) is the difference between the maximum principal stress and the normal traction, which essentially means that where value for the normal traction is greater, the values of the numerator and dilation tendency are accordingly lower. By normalizing the dilation tendency values with the maximum differential stress, they are further scaled to fall in the range between 0 and 1. Dilation tendency values close to 1 thus indicate high potential for dilation and aperture increase, whereas values close to 0 are more indicative of a decrease in aperture.

As in the case of slip tendency, the dilation tendency values are dependent on the relative magnitudes of the principal stresses and this effect is depicted in Figure 8 for the same synthetic stress states as in Figure 7. For low stress ratios, the fractures that have poles in the $\sigma_2 - \sigma_3$ -plane (i.e. fractures that are parallel to the σ_1 -direction) have the highest dilation tendency values and lowest values are found on fractures perpendicular to the σ_1 -direction. For high stress ratios, highest dilation tendency values are found on fractures with poles parallel to the σ_3 -direction, i.e. on fractures that are perpendicular to both the σ_1 - and σ_2 -directions. Thus it can be concluded that, with a progressive decrease in the stress ratio, the pattern that the poles of fractures with high dilation tendency values form, change from a uniaxial cluster around the σ_3 -direction into a uniaxial girdle skewed along the $\sigma_2 - \sigma_3$ plane. The general case in which the greatest dilation is expected to occur on fractures perpendicular to the minimum compressive stress is only found on the special case when the stress ratio is close to 1. Thus, just as in the case of slip tendency, fracture dilation is also highly sensitive to the magnitude of the intermediate stress axis. Similarly too, the number of potentially dilating fractures is much greater and the orientations of such fractures are more diverse for very low stress ratios than for the very high stress ratios.

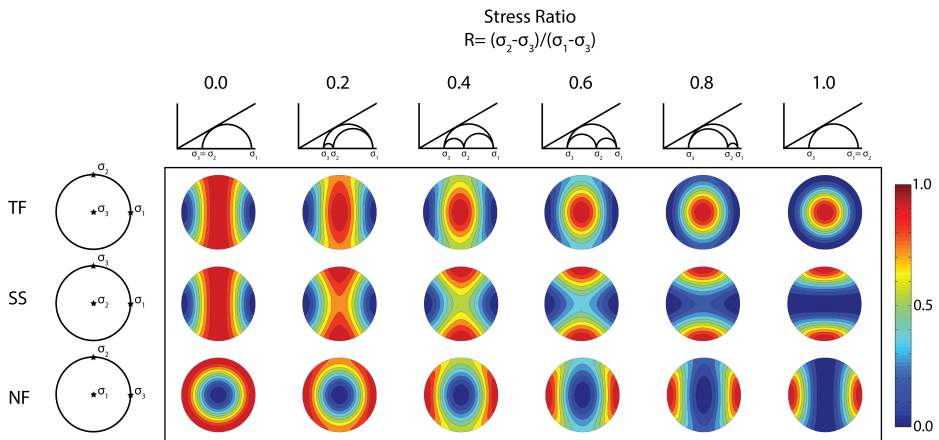


Figure 8: Dilation tendency (T_d) values computed⁴ for all possible orientations in thrust-fault (TF), strike-slip (SS) and normal-fault (NF) regimes with varying stress ratios R . The values are normalized with the maximum differential stress ($\sigma_1 - \sigma_3$) and the value of 1.0 indicates the maximum possible dilation tendency values in the given stress state and value 0 the minimum. Equal area, lower hemisphere projections.

2.3 Paleostress analysis

Paleostress analysis aims at reconstructing past states of stress and their evolution over geological time starting from observations of deformed rocks in the field. In the case of faults, the observations typically require the determination of a so-called fault-slip datum (after Marret & Allmendinger 1990), defined by the orientation of the fault plane, slip direction and sense-of-movement on the fault. In its simplest form, paleostress analysis gives the orientations of the principal stress axes, but more advanced inversion methods also provide information of the relative, though not absolute, magnitudes of the principal stresses. The results of the inversion methods are given in the form of a so-called reduced stress tensor, where the relative magnitudes of the principal stress axes are given in the form of stress ratio:

$$\boldsymbol{\sigma} = \begin{bmatrix} \sigma_1 & 0 & 0 \\ 0 & \sigma_2 & 0 \\ 0 & 0 & \sigma_3 \end{bmatrix} = \begin{bmatrix} 1 & 0 & 0 \\ 0 & R & 0 \\ 0 & 0 & 0 \end{bmatrix} \quad (14)$$

In the equation the reduced stress tensor is given in the principal coordinate system and the maximum principal stress has a nominal value of 1, while the minimum principal stress has a value of 0. The computation of this reduced stress tensor is discussed further in the Section 'Direct inversion methods'.

⁴Computations have been carried out by the Author using MatlabTM

The simplest form of paleostress analysis is based on the Andersonian theory of faulting, which relates the orientations of conjugate faults to orientations of the principal stresses and, assuming that one of the principal stresses is vertical, introduces three simple faulting categories - the thrust, normal and strike-slip faulting regimes (Anderson 1905). Anderson based the foundation of his theory on the analysis of the orientations of planes that carry maximum shear stresses and postulated that thrust faults form with dip angles of $< 45^\circ$ during compression when σ_3 is vertical, normal faults form with dips of approximately $> 45^\circ$ during extension when σ_1 is vertical and subvertical strike-slip faults develop where σ_2 is vertical. Anderson's theory, however, only applies to the specific case of neofomed conjugate faults where the shear stresses are at maximum for two conjugate planes and when the slip is perpendicular to the line of intersection of the faults. Thus, Anderson's theory does not explain oblique-slip faulting or fault patterns deviating from the conjugate system (e.g. Reches 1978) - that is, fault systems deviating from plane strain. In order to derive paleostresses from more complex faulting patterns, more modern methods of paleostress analysis have been developed and these are reviewed further in the following sections, starting first with graphical methods and then proceeding to direct inversion methods. Before advancing further with the topic, it is appropriate to note that each of the paleostress methods rely on the assumptions that individual faults have slipped independently of one other, thus implying that no perturbations of stresses took place during the activation of the faults, no block faulting took place during the faulting, and the material affected by the faulting was continuous, homogeneous, isotropic and linearly elastic (a so-called CHILE material). The methods thus assume that the rock volume that is sampled with the analysed faults is a so-called representative volume and that the stresses derived from the faults are representative as the "average" stress for that volume during the time span when the faults formed or reactivated (Lacombe 2012). More assumptions are also implicit in direct inversion methods and these are reviewed separately below in the relevant section. All of the assumptions related to paleostress analysis are naturally oversimplifications when considering the spectrum of true natural conditions and heterogeneities that may be present in a rock mass at any given time. Critical reviews of the underlying assumptions of paleostress inversion methods have been reviewed critically for example by Twiss and Unruh (1998), Marrett and Peacock (1999), Pollard (2000), Lacombe (2012) and Lacombe et al. (2013).

2.3.1 Graphical stress inversion methods

A wide range of graphical methods have been developed to analyse fault-slip data. I review here two of the most common methods, the so-called P-T-method and right-dihedra method. It is noted that graphical methods are to some extent analogous to the focal mechanism analysis adopted by seismologists, who aim to identify compressional (P-dihedra) and dilatational quadrants (T-dihedra) from the first arrivals of seismic waves and also the centres of these quadrants, which are often named as the pressure (P) and tension (T) axis.

When the orientation of the fault plane, the direction of the slip lineation and the sense of movement on the fault plane are known, it is possible to use a so called P-T-method to analyse principal axis of average incremental strain, based on the identi-

fication of kinematic shortening (P) and extension (T) axis for each fault (Turner 1953, Marret & Allmendinger 1990). The method assumes that both the shortening and extension axis are located within a 'movement' plane defined by the slip direction and the normal to the fault plane and at an angle of 45° from these poles; the mutual locations of the shortening and extension axes are defined by the sense-of-slip of the fault (Figure 9). If the sense of slip is reversed, then the mutual locations of the shortening and extension axis are also switched respectively. By contouring of the kinematic axis for a larger number of kinematically compatible faults, it is possible to characterize the orientations of the average principal axes of the incremental strain tensor (Marret & Allmendinger 1990) or the instantaneous strain axis during simple shear (Fossen 2010), which, in a broad manner, may be interpreted as representing the average orientations of principal stress axes. It is however already obvious from the Coulomb failure law, that one should be careful in assuming coaxiality between the strain and the stress axes - based on Coulomb's law and the frictional properties of rock (e.g. Byerlee 1978), one should expect the σ_1 direction to be at an angle of 30 to 40 degrees from the fault plane instead of the assumed 45 degrees. Nevertheless, the P-T-method has been shown to yield results similar to those obtained by more advanced stress inversion methods and which are also compatible with known stress orientations (e.g. Blenkinsop 2006, McGarr & Gay 1978).

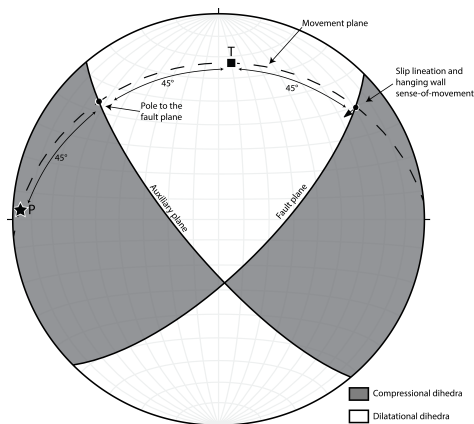


Figure 9: An example of the identification of kinematic shortening (P) and extension (T) axis for a fault-slip datum. The kinematic axis, the pole to the fault plane and the slip direction are located in a common 'movement' plane, at an angle of 45 degrees to the slip direction and pole to the fault plane. The mutual locations of the kinematic axis are determined by the sense-of-movement of the fault plane. Equal area, lower hemisphere projection. The arrow shows the relative movement direction of the hanging-wall block with respect to the footwall block.

The right dihedral method is a very similar approach to the P-T method for estimating paleostresses from fault-slip data (e.g. Angelier & Mechler 1977, Angelier 1994, Marret & Allmendinger 1990, Ramsay & Lisle 2000). In this method, the lower hemisphere projection is first divided into compressional and dilatational quadrants (di-

hedra) by the use of two orthogonal planes - the fault plane and a so-called auxiliary plane, perpendicular to the slip direction and the fault plane (Figure 9). The nature of each quadrant is then determined by the orientations of the shortening and extension axis - shortening axis is located in the compressional quadrant and extension axis in the dilatational quadrant, respectively (Figure 9). It may further be interpreted that the principal stress axis σ_1 is located within the compressive dihedra and σ_3 within the dilatational dihedra. The right-dihedra method thus provides “ranges” for the feasible orientations of the principal stress directions. For faults formed in a uniform stress regime, the principal stress axis must locate in the corresponding dihedra, and as a consequence, by superimposing the right-dihedra representations of multiple fault-slip datum, it possible to reduce the size of dihedral fields and the potential orientations of the stress axis (Figure 10).

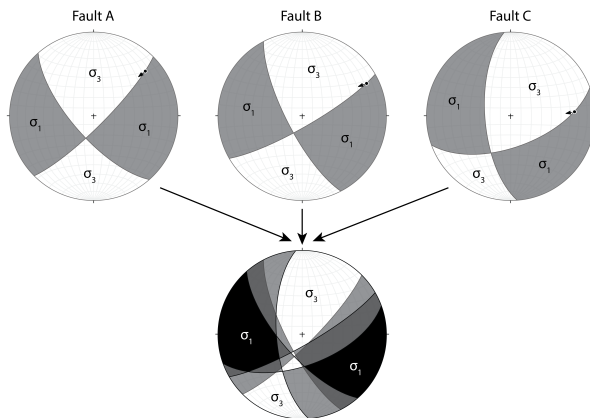


Figure 10: An example of the use of the right-dihedra method to constrain the principal stress axes from a small population of faults assumed to have formed in the same stress regime. The dihedra of three individual faults (Fault A, B and C) are superimposed in order to reduce the size of the compressional and dilatational dihedra and thus to constrain the potential orientations of the principal stress axes. The reduced compressional dihedra are shown in black and dilatational dihedra in white in the lowermost stereonet.

Graphical methods do not generally constrain the relative magnitude of the principal stress axes or the stress ratio and hence cannot be used to evaluate the full form of the reduced stress tensor. However, according to Angelier (1994), the distribution of the reduced right-dihedra domains can yield general information on the approximate stress ratio values, although he did not discuss this topic any further in his paper. This concept was further developed by Delvaux & Sperner (2003), who introduced an “Improved Right Dihedron Method”, which employs numerical analysis of reduced dihedra to estimate the stress ratio for a given population of faults. The method,

however, is only applicable to large fault populations having a large spread in fault orientation and can thus only be applied in regions with good exposures and statistically rich fault-slip data.

In spite of the obvious limitations of the graphical paleostress methods, they can be used to gain first-order estimates of the orientations of the principal stress axes and, more importantly, as a first method for differentiating heterogeneous datasets of faults into mechanically compatible subpopulations. These subpopulations can then be further analysed with the direct inversion methods.

2.3.2 Direct inversion methods

All direct inversion methods are based on the assumption that the slip direction on a fault is parallel to the maximum resolved shear traction (Wallace, 1951, Bott, 1959). From this principle the inversion methods aim to find a best-fit stress tensor that is most compatible with the field observations of faults and their slip directions. Several different types of inversion methods have been developed (e.g. Angelier 1979, Angelier 1984, Etchecopar et al. 1981, Yamaji 2000, Delvaux & Sperner 2003). Invariably, their aim is to find a stress tensor that minimises specific object functions that describe the fit of the computed tensor by applying either iterative or grid-search methods. In most inversion algorithms the function to be minimised describes a so-called misfit angle (Figure 11), which is the angle between the theoretical shear traction vector and the measured slip directions (Angelier 1979, 1984, Carey 1976, Etchecopar et al. 1981, Lisle 1988), but along with the minimisation of the misfit angles, some methods also try to maximise the relative magnitudes of shear tractions on the fault planes (Angelier, 1990, Delvaux & Sperner, 2003). The success of the inversion is analysed statistically with the sum of the object function, which should thus reach a minimum value during the inversion process.

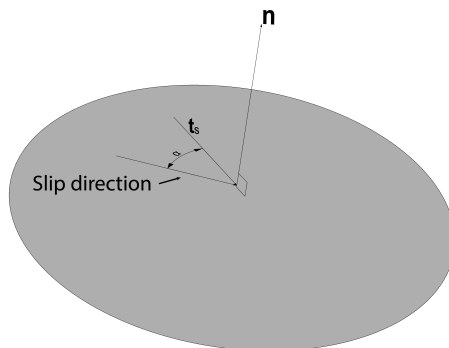


Figure 11: Misfit angle α is the acute angle between the slip direction and the shear traction vector t_s . Inversion methods aim to minimise, either through a grid-search or iterative processes, object functions, which usually are a function of the misfit angle.

As inversion methods are based solely on the orientations of fault planes and of

the associated slip directions, the results computed from the inversion cannot include any information on the stress magnitudes. For this reason, the analysis of paleostresses through inversion does not permit the definition of the complete stress tensor but, instead, the results are limited to the reduced tensor (Angelier 1994), given in Equation (14). The reduced stress tensor is composed of three variables specifying the orientations of the principal stress axes and a fourth variable, the stress ratio. Given that the reduced stress has four unknown variables, in theory only four independent fault-slip measurements are needed to solve the reduced stress tensor. In order to get statistically reliable results, however, Orife & Lisle (2006) recommended using at least eight fault-slip data measurements and Hippolyte et al. (2012) anything between ten and twenty measurements or even more in rock masses recording polyphase faulting events.

Inversion is typically iterative or exploratory process, where the fault-slip data are tested with numerous tensors and the fit of each tensor is compared through the analysis of the object function. This process is exemplified in Figure 12 where a synthetic fault-slip data set is analysed by a direct inversion method using a function to minimise the misfit angles between the observed and theoretical slip vectors. In Figure 12A, all the faults are analysed as a single population and the corresponding best-fit tensor and the resulting misfits are shown. Ideally, the misfit distributions should show monotonously decreasing behaviour but in the case of Figure 12A, there are also some high-values associated with the faults, which may indicate that the faults consist of two fault populations formed in different stress regimes. Consequently, based on their geometries, the faults have been divided into two geometrically more homogeneous groups and re-analysed again with the inversion method, which this time results in a much better fit and more ideal misfit distributions (Figure 12B,C). This highlights the importance of the separation of fault subsets from heterogeneous data - ideally this should be done by using field criteria, such as successive striations, mineral paragenesis and crosscutting relationships (Viola et al. 2009, Hippolyte et al. 2012, Angelier 1994) albeit automated methods have also been developed (e.g. Delvaux & Sperner 2003, Yamaji 2000, C  lerier 1995).

It is noted that with the use of the direct inversion, the stress ratio, and thus the reduced stress tensor, cannot be properly constrained in the case when the fault-slip data does not contain oblique-slip faults (Hippolyte et al. 2012, Angelier 1994). In the case of ideal conjugate faults, the shear stress does not change with the stress ratio as the intermediate stress axis is always parallel to the intersection of the faults and thus slip occurs on the plane defined by σ_1 and σ_3 , irrespective of the relative magnitude of σ_2 (Hippolyte et al. 2012). Consequently, in order for the inversion to work, some heterogeneity in the fault-slip data must occur.

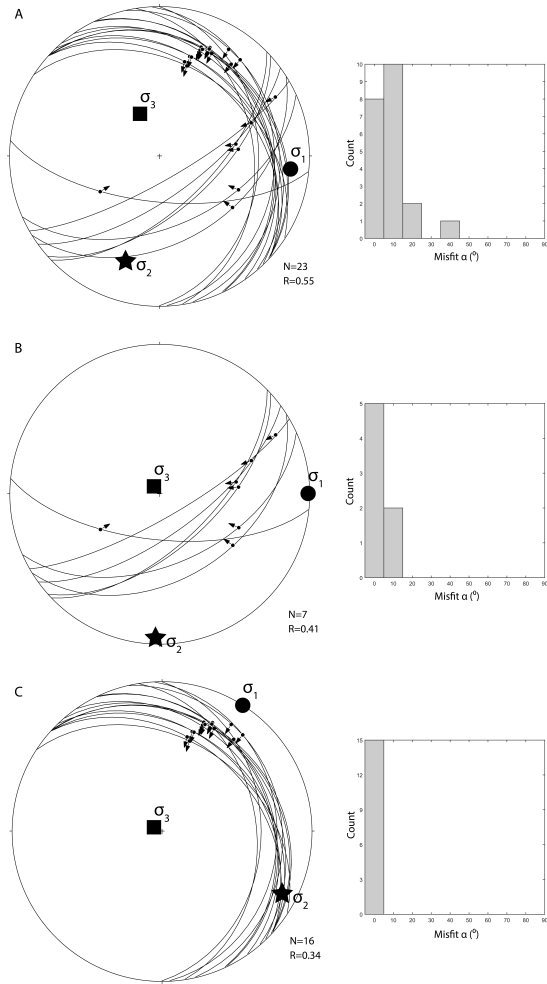


Figure 12: An example of an inversion procedure for the synthetic fault-slip data set shown in A. In A, a best-fit tensor is shown together with the misfit histogram, indicating that the applied tensor is not an ideal solution. In B and C, the original data set is separated into homogeneous subgroups that are mechanically more consistent than the original group population. The misfits in B and C show ideal distribution with monotonically decreasing behaviour, suggesting that the applied tensor can be considered as a good solution. Usually only misfit angles less than 30 degrees are accepted during the inversion procedure (e.g. Delvaux & Sperner 2003).

3 Review of the original publications

Paper 1: New constraints on 1.7 Gyr of brittle tectonic evolution in southwestern Finland derived from a structural study at the site of a potential nuclear waste repository (Olkiluoto Island)

The aim of this paper was to reconstruct the evolution of faults and fractures through time at Olkiluoto Island and to constrain the paleostress regimes that have affected Olkiluoto Island and southwestern Finland since the bedrock first attained conditions favourable for brittle deformation. The analysis was based on an extensive fault-slip database collected from the site during site investigations at Olkiluoto and complementary fracture and fault-slip data collected from outcrops. Through paleostress inversion of fault-slip data from rock units of different ages it was possible to distinguish seven distinct paleostress states that have affected Olkiluoto region. These were, from oldest to youngest: (1) NW-SE to NNW-SSE transpression, which acted soon after 1.75 Ga, when the presently exposed crustal level had cooled sufficiently such that response to stress was predominantly brittle in character followed by (2) N-S to NE-SW transpression, which caused partial reactivation of structures formed in the first event; (3) NW-SE extension during the Gothian orogeny and at the time of rapakivi magmatism; (4) NE-SW transtension that occurred between 1.60 and 1.30 Ga and which also formed the NW-SE-trending Satakunta graben located some 20 km north of Olkiluoto; (5) NE-SW compression that was found to postdate both the formation of the 1.56 Ga rapakivi granites and the 1.27 Ga olivine diabase sills, which also intruded the Satakunta graben; (6) E-W transpression during the early stages of the Mesoproterozoic Sveconorwegian orogeny and which also predated (7) almost coaxial E-W extension attributed to late Sveconorwegian orogenic collapse. By further analysis of the orientations of the fault and fracture populations that were active during these different stress regimes, together with an assessment of the variability of the stress ratios deduced from the paleostress data considered to represent these different stress regimes, we concluded that the phase of crustal fragmentation, i.e. the period during which new faults and fractures were formed in the Olkiluoto bedrock, was relatively brief compared to the subsequent phase of 'jostling', i.e. to the phase of reactivation of old structures. The bedrock at Olkiluoto and southwestern Finland had thus already attained a high level of structural maturity during relatively early phases of the evolution of the crust. By comparing our results with those of similar analyses conducted at Sweden, we recognized remarkable similarities in the evolutionary sequence of brittle structures in the two areas. On this basis, we proposed to imply that at least the southern part of the Fennoscandian Shield had reached such structural maturity during Mesoproterozoic, after which the Shield behaved as a more or less coherent rigid craton, deforming mostly through reactivation of pre-existing structures. This also implies that any future stress changes are most likely to be accommodated by the reactivation of existing brittle structures rather than by the generation of new ones.

Paper 2: K-Ar illite age constraints on the Proterozoic formation and reactivation history of a brittle fault in Fennoscandia

The purpose of the paper was to determine the age and timing of potential reactivation of a major fault located at Olkiluoto. The core of the fault consisted of two distinct and texturally different components - a finer grained, ultracataclasite- and gouge-bearing section, which also formed injection-like apophyses into a slightly coarser gouge located in the same fault core section, suggesting a younger age for the finer-grained component. By digital image analysis of impregnated gouge samples of both components, we were able to confirm that the mean grain size of the first gouge sample was indeed finer than that of the other sample, suggesting more pervasive grain size comminution and a more intense strain history, which was also consistent with the postulated younger age. By K-Ar dating of authigenic, synkinematic illites from different grain size fractions, we were able to show that the ages of the fine-grained sample were consistently younger than those of the coarser-grained sample, which also confirmed the age relation assumed from the macroscopic textural relationship and the microscopic grain size distributions. The finest grain size fractions ($< 0.1 \mu m$) considered to represent authigenic illites, yielded an age 886 ± 18 Ma, which is accordingly interpreted as recording the most recent faulting episode, while an age of 1006 ± 21 Ma was obtained for the coarse-grained sample. By combining the age data with the results of paleostress analysis of fault-slip data from the fault, we were able to link the faulting episodes to the E-W shortening during the contractional phase of the Sveconorwegian orogen and E/ESE-W/WNW extension during the collapse of the orogen. The results of the paper thus provide direct evidence of Proterozoic brittle activation and reactivation within a single fault, separated in time by more than 300 Ma, and also extreme strain partitioning within a relatively narrow fault core.

Paper 3: Stress-controlled fluid flow in fractures at the site of a potential nuclear waste repository, Finland

The scope of the study was to assess whether the fluid flow in fractures at Olkiluoto is controlled by the in-situ stresses by combining fracture orientation data with stress and flow measurements carried out at Olkiluoto Island during the detailed site investigations. The present day stresses at Olkiluoto indicate a thrust faulting regime, with the maximum principal stress oriented approximately E-W in the uppermost 300 m depth of the bedrock, WNW-ESE at 300-500 m depth and again approximately E-W at depths below 500 m. The changes in stress orientations may be associated with the occurrence of major low-angle faults, which coincide approximately with the depths where the stress orientations change. The stress ratios also change with depth and in the upper part pure thrust regime with a stress ratio of 0.6 prevails, while in the deeper parts the regime changes toward a transpressive regime, indicated by a stress ratio of 0.1. In order to test whether flow in the fractures is controlled by the in-situ stress, we compared the orientation distribution of the transmissive fractures to the distributions predicted from slip and dilation tendency analysis. Based on the comparison, we could conclude that the fracture orientations have a remarkable correlation with the predicted normalized dilation tendency values at different depths. This indicates that the flow is controlled

by normal tractions instead of the criticality of the fractures. By further comparing the transmissivity values of the fractures with absolute normal and shear traction values, it was possible to show that there is a general tendency for the transmissivity values to decrease with increasing normal tractions, whereas no trends in transmissivities could be observed for the increasing or decreasing shear traction values. Based on the results we concluded that at Olkiluoto the flow in fractures is controlled by dilation and emphasized the importance of normal traction instead of fracture criticality for fracture flow. We also concluded that the orientations of relative transmissivities of conductive fractures may be predicted by combining in-situ stress data with slip and dilation tendency analysis. A prerequisite for such analysis is however a full stress tensor instead of using two-dimensional approximations of the stress state.

Paper 4. Brittle tectonic evolution along the western margin of South Africa: More than 500 Myr of continued reactivation

The purpose of the study was to present a conceptual scheme for the more than 500 Ma brittle deformation history of the Namaqualand region of western South Africa, by combining remote sensing and field studies. The field data consisted of fault-slip data collected from rock units of different ages and with distinct crosscutting relationships. The remote sensing data was used to identify prominent fracture and fault sets with systematic trends and consistent geometric relationships, e.g. conjugate faults. These were used in the assessment of principal stress orientations during the formation of the structures and for the comparison with observed crosscutting relationships. Analysis of the combined data enabled the recognition of up to ten brittle deformation phases, spanning in time from Neoproterozoic to Cenozoic. The brittle evolution of the study area commenced with the generation of steep NNW-SSE oriented strike-slip faults during the Neoproterozoic Pan African orogeny. Subsequent deformation was mostly expressed by the reactivation of these pre-existing structures, indicated for example by the presence of similarly oriented faults bearing slip striations with significantly different orientations. Based on these observations, we attributed this to a progressively decreasing ratio between crustal fragmentation and jostling with time. In other words, the structural maturity of the study area prevented the nucleation and development of new brittle structures with orientations other than the overall NNW-SSE grain, inherited from the early Neoproterozoic deformation events. By using the in-situ stresses we were also able to show that the crust in the study area is in a state of frictional equilibrium. Slip tendency analysis further showed that the NNW-SSE oriented steep structures and their WNW-ESE oriented conjugate faults are the most prominent candidates for reactivation in the present day stress state, which is also in agreement with the observed present day seismicity. The results of analysis of the paleostresses and present day stresses, in conjunction with the orientations of the faults of different deformation episodes consequently show that brittle deformation in Namaqualand has been, and continues to be, predominantly controlled by the reactivation of the Neoproterozoic NNW-SSE oriented steep strike-slip faults.

4 Discussion

4.1 Crustal evolution of southwestern Finland

The evolution of the Finnish bedrock after the Svecofennian orogeny and in particular the development of the brittle structures is relatively poorly constrained and most existing studies focusing on the topic have only established ages and kinematic constraints for the waning stages of the Svecofennian orogeny (e.g. Torvela & Ehlers 2010, Torvela et al. 2008, Väisänen & Skyttä 2007, Saalman 2007) or, in a few studies, on Gothian and Jotnian events (Elminen et al. 2008, Elminen et al. 2006, Mertanen et al. 2001, Heeremans & Wijnrans 1999, Ploegsma 1991). Thus the results of this thesis and the underlying papers (Papers I-III) provide new insights and constraints on the crustal development of the southwestern Finland after the Svecofennian orogeny. The conclusions concerning the evolution of the brittle deformation (Paper I) further provides a conceptual scheme against which new observations may be compared and the validity of the scheme tested.

The proposed conceptual scheme is divided into seven distinct stages. Brittle deformation of the presently exposed crustal level in southwestern Finland is considered to have begun approximately 1.75 Ga ago with the formation of conjugate NNW-SSE and NE-SW striking strike-slip faults and synkinematic reactivation of SE-dipping low-angle shear zones and foliation planes during NW-SE to NNW-SSE compression (Paper I). The analysis of stress ratios derived from paleostress analysis in Paper I further indicates that this stage was mostly characterised by transpressive stress conditions, corroborating the simultaneous activation and reactivation of vertical and low-angle structures. The results given in Paper I show similarities with observations made by Torvela & Ehlers (2010) from shear zones in southern Finland and may also reflect the stress conditions of the waning stages of the Svecofennian orogeny. The late stages of the Svecofennian orogeny is considered to be a result of a continent-continent collision juxtaposing Sarmatia and Fennoscandia at approximately at 1.84 Ga (Elming et al. 2001, Lahtinen et al. 2005), leading to N-S shortening and further NW-oriented thrusting in transpressive conditions (Ehlers et al. 1993). NW-oriented contraction was also suggested by Väisänen & Skyttä (2007) who concluded that in southern Finland the evolution further resulted in the development of E-W oriented strike-slip shear zones and N-S oriented reverse shear zones within transpressional stress regime. There are strong similarities between the model proposed by Väisänen & Skyttä (2007) and the conditions of the Stage 1 proposed in Paper I. It is tentatively proposed that the stage reflects the continuation of the stress conditions generated during the continent-continent collision at ca. 1.84 Ga, which further evolved into transpressional conditions leading to the formation of the major shear zones in southern Finland and the structures observed at Olkiluoto. Similarities with the inferred stress conditions and observed brittle structures in southeastern Sweden (Viola et al. 2009, Saintot et al. 2011) also suggest that the stresses were sustained throughout the southern portion of Fennoscandian shield and, considering the time frames, the NW-SE to NNW-SSE shortening could have been sustained for a period for at least 100 Ma. The Stage 2 deformation event (Paper I) is considered as an indication of a clockwise rotation of horizontal stress components in southern Finland, leading to an episode of N-S to NE-SW compression in transpressive

environment and reactivation of the structures formed during Stage 1. Saalman (2007) and Saalman et al. (2009) documented similar post-Svecofennian stress rotation from southern Finland.

Gothian stage and the formation of rapakivi granites and diabase dikes in southern Finland are generally associated with overall extensional crustal setting (e.g. Rämö & Haapala 2005, Korja et al. 2001) and such extension is also supported by the several stress tensors obtained from paleostress inversion and the existence of NE-SW oriented diabase dikes at Olkiluoto - these support the notation of NW-SE oriented extension (Stage 3 of Paper I) at Olkiluoto and thus a switch from the N-S to NNE-SSW compression of Stage 2 to extensional setting. Väisänen & Skyttä (2007) tentatively proposed that a regional E-W extension may have taken place prior to the rapakivi magmatism, at the time of the 1.79-1.77 Ga orogenic collapse suggested by Lahtinen et al. (2005). Based on the results of Paper I, it is however proposed that the E-W extension may also be associated with the extensional phase documented here and was still active at least during the formation of the diabase dikes and rapakivi granites. Further, at Olkiluoto the initiation of the extension was preceded by the transpressional stages postulated to have started at 1.75 Ga (Paper I), potentially constraining also the age for the regional extension proposed by Väisänen & Skyttä (2007) and either questioning the time of onset of the orogenic collapse or suggesting that at Olkiluoto the collapse was expressed by transpressive deformation. The greisen-type veins occurring in the Olkiluoto region and associated with the cooling phase of the rapakivi granites, together with several stress tensors indicate further evolution of the stress state and rotation of the extension direction from a NW-SE direction during Stage 3 to NE-SW, which is consistent with the opening direction of the ca. 1.6-1.3 Ga aged Satakunta graben, located north of Olkiluoto. The NE-SW extension is associated with Stage 4 (Paper I) and is characterised by transtensional stress regime and the reactivation of both low-angle structures and subvertical strike-slip faults. A new insight of this thesis and Paper I is the identification of a NE-SW oriented compression (Stage 5 of Paper I) postdating the rapakivi granites and the Postjotnian olivine diorites and it is also suggested that this compression may have led to the inversion of the Satakunta graben, possibly explaining the observations of tilted sandstone beds (Kohonen & Pihlaja 1993) and open to gentle NNW-SSE trending folds observed within the sandstone layers (Pajunen & Wennerström 2010). Due to lack of evidence, however, it is noted that such structures may have developed syn-extensionally.

The data from Olkiluoto suggest an episode of near E-W compression (Stage 6 of Paper I), which, based on its orientation and K-Ar ages derived from gouges associated with kinematic data compatible with this phase, is assigned to the early stages of the Sveconorwegian orogeny, at 1.14 Ga (e.g. Bingen et al. 2008, Paper II). Similarly oriented compression directions have also been documented by Viola et al. (2009) and Saintot et al. (2011) from southeastern Sweden and it is suggested that far-field stresses of the Sveconorwegian orogeny were accommodated in southwestern Finland through the reactivation of favourably oriented brittle structures. The Sveconorwegian orogeny was followed by a phase of orogenic collapse (e.g. Bingen et al., 2008; Viola et al., 2009, 2011) and approximate E-W extension is well documented for the late phases of the Sveconorwegian orogeny from southeast Norway (e.g. Viola et al., 2011) and southern and southwestern Sweden (e.g. Viola et al., 2011, Viola et al. 2009 and Saintot et al.

2011). This phase is interpreted as having affected Olkiluoto as some tensors derived from favourably oriented low-angle reactivated faults record normal dip-slip movements (Stage 7 of Paper I); late Sveconorwegian K-Ar ages have also been obtained from gouges from faults mechanically compatible with this stage (Paper II). It is noted that several N-S trending, as yet undated, diabase dykes have been documented to crosscut the olivine diabbases of the Satakunta region (Vorma & Niemelä 1994, Veräjämäki 1998, Amantov et al. 1996), but whether these have formed during Sveconorwegian E-W extension accompanying the collapse of the Sveconorwegian orogeny is still unresolved. The age of these dykes should be determined in order to test this hypothesis.

4.2 Structural maturity

The evolution of a crust in the brittle regime can be assigned to phases of fragmentation, i.e. activation or generation of new brittle structures, and jostling, i.e. reactivation of existing structures (Munier & Talbot 1993). There is a general tendency for the ratio between activation and reactivation to decrease with time as the crust becomes saturated with brittle structures, formed under varying stress conditions, or as stated by Munier & Talbot (1993), as the "orientation spectra" of fractures widens. Thus, instead of generating new fractures, the stresses are accommodated by reactivation of fractures with favourable orientations with respect to the stress state, and with the advent of several fracture sets with different orientations, reactivation becomes the main mode of deformation. In Paper I, such a phase of fracture saturation is referred to as structural maturity. Munier & Talbot (1993) showed that such an evolutionary trend can indeed be recognized by analysing the development of fractures in southeastern Sweden and concluded that by mid-Paleozoic time, deformation of the crystalline basement was mostly accommodated by reactivation of pre-existing structures. Similar developments can be demonstrated for the bedrock of southwestern Finland (Paper I) as the data from Olkiluoto show that after the formation of the Subjotnian diabbases at 1.27 Ga (Suominen 1991), stresses were accommodated by the reactivation of pre-existing fractures instead of generation of new ones. This shows further that the activation phase was relatively short compared to the reactivation phase, only 500 Ma compared to the 1.75 Ga period of brittle conditions. Similar results have been obtained from southern Sweden (Viola et al. 2009, Saintot et al. 2011) which implies that, after the Svecofennian orogeny the southern part of the Fennoscandian shield behaved as a coherent rigid crustal body and accommodated far-field stresses in a comparable manner, and attained structural maturity with respect to brittle structures during the Mesoproterozoic era. Due to this structural maturity of the crust, it is possible to predict that future stress changes will be mostly accommodated by reactivation of existing structures and the probability of formation of new large-scale structures can be considered low. An example of Neoproterozoic reactivation is given in Paper II, where Neoproterozoic reactivation of a single fault is shown to have taken place through extreme strain localisation within a narrow band of Mesoproterozoic fault gouge. To our present knowledge, this example is the first successful isotopic dating of a reactivation event within a single fault core and adheres to the concept of structural maturity.

The Namaqualand region in South-Africa shows similar crustal evolution with respect to the activation and reactivation (Paper IV). Structural maturity of the bedrock

was reached relatively soon after the formation of first brittle structures during the Neoproterozoic, after which the brittle deformation at Namaqualand was controlled by the reactivation of pre-existing steep strike-slip faults. This reactivation continues also during present day, as indicated by the present-day seismicity. In Paper I it is also suggested that the variability in the stress ratio values derived from paleostress inversion can be used as a potential proxy for the amount of activation vs. reactivation. Large variability in the stress ratio values can reflect the reactivation of a number of fracture populations with varying orientations and is an indication that far-field stresses are locally perturbed with respect to the relative magnitudes of the principal stresses due to pre-existing structures in the bedrock. It is noted, however, that further work is needed to validate of use of the stress ratio as a proxy for the ratio between activation and reactivation and at the moment the idea is considered as a working hypothesis.

4.3 Fluid flow along fractures

When the coupling between in-situ stress and fluid flow along fractures is considered, the criticality of fractures is a widely accepted proxy for fluid flow. This concept is supported by numerous studies, suggesting that flow is concentrated on fractures that are on the verge of failure (e.g. Rogers 2003, Townend & Zoback 2000, Ito and Zoback 2000, Barton et al. 1998, Hickmann et al. 1997, Barton et al. 1995). Some other studies have alternatively highlighted the importance of low effective normal tractions (e.g. Heffer & Lean 1993). At Olkiluoto, approximately 6 % of all the fractures are transmissive and the distribution of the orientations of the transmissive fractures deviates from those of the non-transmissive fractures; based on statistical analysis, this cannot be explained simply by random sampling from the population of the non-transmissive fractures (Paper III). By using slip and dilation tendency analysis, it was shown in Paper III that the orientations of the transmissive fractures correlate with the distribution of highest dilation tendency values (lowest normal tractions) and, furthermore, highest transmissivity values correlate with lowest normal traction values. Thus, at Olkiluoto the fluid flow along fractures is coupled with normal tractions, contradicting the concept of critically stressed fractures. The data from Olkiluoto represents rather shallow conditions (< 1 km) compared to the provided data supporting the coupling fluid flow and fracture criticality, with sampling depths up several kilometers (e.g. Ito and Zoback 2000, Barton et al. 1998, Hickmann et al. 1997, Barton et al. 1995) and one explanation for the seemingly contradictory results from different locations may be related to the effect of depth. According to the combined Griffith-Coulomb failure law, shear fracturing is driven by large differential stresses, which can only be sustained at great depths (e.g. Townend & Zoback 2000), whereas tensile fracturing takes place at low differential stresses, which typically occur close to the surface (Sibson 1994). Tensile fracturing takes place when the Griffith failure criterion is met:

$$t_s^2 + 4Tt_n - 4T^2 = 0 \quad (15)$$

where T is the tensile strength of the rock. In order for tensile fracturing to take place, the differential stress ($\sigma_1 - \sigma_3$) needs to be less than $4T$ and this failure condition is

depicted in Figure 13, together with conditions leading to shear failure. When the differential stress is larger than $4T$, shear failure becomes the main mode of failure. Although it is acknowledged here that the Griffith-Coulomb failure law only applies to failure in pristine rock, it does however consider the role of cohesion, which is typically neglected in the concept of critically stressed fractures. As the depth increases, together with the prevailing differential stress, the effect of cohesion can be considered very small, but in shallow conditions and for low differential stresses, it may have an important role in the reactivation of pre-existing fractures. The potential depth where reactivation changes from tensile deformation, i.e. dilation, into shear deformation can be roughly estimated from the Griffith-Coulomb failure law by assuming that the differential stress is equal to $4T$, σ_3 is equal to the lithostatic load (and thus vertical, reflecting the thrust stress regime conditions of Olkiluoto) and that the ratio of σ_1 to σ_3 is ca 2.3, defined by assuming that the crust is in frictional equilibrium and that the ratio is constrained by the Coulomb failure curve (Harrison et al. 2007). Thus the following equation can be established for the depth Z :

$$z = \frac{4T}{1.3\rho g} \quad (16)$$

where ρ the density of the rock and g the gravitational acceleration 9.81 m/s^2 . For the values of $T=10 \text{ MPa}$ (estimated average value for the rocks at Olkiluoto, Posiva 2011) and $\rho=2700 \text{ kg/m}^3$, Z equates to a depth of ca. 1.2 km . The results thus shows that at shallow conditions, at depths of say less than 1 km , the Griffith failure law can be considered valid and the mode of deformation for fractures is opening or dilation rather than shear failure, which prevails at larger depths and is driven by larger differential stresses which cannot be sustained close to the surface. Shear deformation can however take place even at lower differential stresses when the cohesion of the fractures is very low, but considering that at Olkiluoto, no shear deformations or microseismicity within shallow fractures have been observed (e.g. Johansson & Siren 2014), it can be speculated that either the cohesion of the fractures is high or the fracture system at shallow conditions forms a locked network that inhibits shear deformations (corresponding to a situation of high cohesion), thus promoting dilation due to low normal stresses. Such conditions are also likely to occur in general in other areas where structural maturity has been attained and the bedrock has been saturated with fractures in different orientations. The results of Paper III are consequently held valid for shallow conditions, whereas fluid flow in fractures is promoted through fracture criticality at greater depths, as shown for example by Townend & Zoback (2000), Ito and Zoback (2000), Hickmann et al. (1997) and Barton et al. (1995). The importance of low normal tractions at shallow depths ($< 1 \text{ km}$) was recently elaborated by Earnest & Boutt (2014), supporting the conclusions given here. The coupling of fluid flow along fractures and in situ stresses can also be considered as another example of fracture activation and reactivation, manifested either through dilation or shear deformation, the mode of reactivation depending on the depth as shown here.

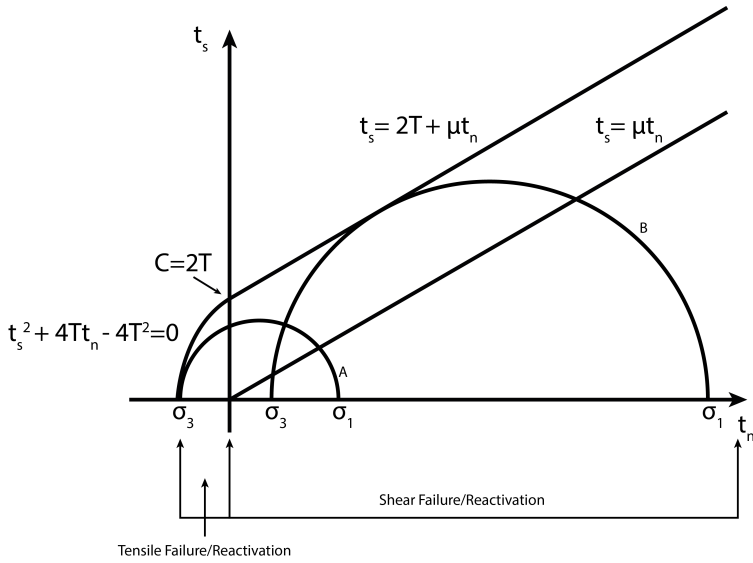


Figure 13: Mohr circles depicting differential stresses that lead to (A) tensile and (B) shear failure/reactivation, depending in the values of cohesion, C , and friction coefficient μ .

4.4 Implications for seismicity

From a simple perspective, earthquakes occur on zones that are most suitably oriented for slip, that is, on zones having shear traction values exceeding the frictional strength of the zone. As a consequence, high slip tendency values can be considered as a proxy for potential earthquake hosting zones as shown in Paper IV and e.g. in Collettini & Trippetta (2007). At Namaqualand in western South Africa, faults that were formed already during the Neoproterozoic and having high slip tendency values in current situ stresses were shown in Paper IV to be the loci of present day seismicity, conforming to the concept of reactivation as the main mode of deformation in structurally mature settings. Albeit Olkiluoto is shown to be barren of seismicity by historical seismic catalogues (Saari 2013), the cataclastic injection vein documented in Paper III can be considered as an fluidized fault rock and an indication of a paleoseismic event (e.g. Ujiie et al. 2007, Rowe et al. 2005, Lin 2011, Rowe et al. 2012), that took place at 886 ± 18 Ma ago, during the collapse phase of the Sveconorwegian orogeny. The earthquake occurred on a fault that was either activated or reactivated during the main phase of the Sveconorwegian orogeny at 1006 ± 21 Ma, thus evidencing multiple reactivations within a single fault and showing that the fault was favourably oriented for reactivation both in E-W compression and E-W extension. The two examples provided here suggest that in structurally mature settings such as Namaqualand and Olkiluoto, seismicity is controlled by pre-existing structures favourably oriented with respect to

prevailing stress states and as the crust of such settings is more or less saturated with fractures in different orientations, the main mode of deformation is reactivation rather than activation, as originally suggested by Munier & Talbot (1993). Favourably oriented zones for reactivation can further be identified by slip tendency analysis, given that the stress conditions are known.

5 Conclusions

The main conclusions of this thesis are summarized in the following bullet points:

1. A brittle deformation scheme for Olkiluoto is presented and this shows seven distinct stress regimes that span from late Svecofennian times into Sveconorwegian collapse. The earliest brittle structures formed at ca. 1.75 Ga in a transpressive regime with overall NE-SW directed compression. The stress state at this stage is considered as a continuation of the stresses prevailing during the waning stages of the Svecofennian orogeny. The main compression direction later rotated clockwise to a N-S direction and caused the reactivation of pre-existing structures.
2. During the Gothian time, NW-SE extension took place and NE-SW oriented diabase dikes intruded into the bedrock. This was followed by extension in a NE-SW direction within an overall transtensional stress regime, reactivating both low-angle structures and subvertical strike-slip faults. At this stage, rapakivi granites, greisen veins and the Satakunta graben were also formed.
3. After the formation of rapakivi granites and the 1.26 Ga olivine diorites, a hitherto undocumented phase of NE-SW oriented compression in a transpressive setting took place, which may also have caused inversion of the Satakunta graben.
4. Sveconorwegian orogeny is documented by E-W compression and followed by E-W extension during the collapse of the orogeny. During this phase, pre-existing structures were reactivated and one of these reactivations is manifested by a paleo-earthquake that is dated at 886 ± 18 Ma.
5. The data from Olkiluoto and Namaqualand shows that the crust at both sites is structurally mature and thus saturated with fractures formed at different periods of time. At Olkiluoto, the structural maturity was reached already during the Mesoproterozoic, thus indicating that the phase of fracture generation was relatively short compared to the phase of fracture reactivation. By comparison with data from southern Sweden, it is possible to conclude that after the Mesoproterozoic, the whole of the southern Svecofennian crust behaved as a coherent rigid crustal body and accommodated far-field stresses in a comparable manner. Due to this maturity, it can also be expected that the any stresses (current or future) are accommodated through the reactivation of favourably oriented pre-existing structures rather than by the generation of new fractures.
6. Fluid flow along the fractures at Olkiluoto is coupled with low normal tractions caused by the in-situ stresses and thus deviates from the generally accepted critically stressed fracture concept. It is suggested that the difference is caused by the shallow conditions and low differential stresses at Olkiluoto - due to the low differential stresses, fracture activation and fluid flow is controlled by dilation due to low normal tractions. At deeper settings, however, fluid flow is controlled by fracture criticality caused by large differential stresses, which drive shear deformation instead of dilation.

7. Both at Olkiluoto and Namaqualand, seismicity is driven by the reactivation of pre-existing structures that are favourably oriented with respect to prevailing stresses. At Namaqualand, this is shown for present day seismicity and at Olkiluoto, for a Neoproterozoic earthquake reactivating a fault that formed at latest during the Mesoproterozoic. In structurally mature settings, seismic events are likely to occur in pre-existing zones that are favourably oriented with respect to prevailing stresses and such zones can be identified through slip tendency analysis, given that the stresses are known.

Acknowledgements

“Nothing in life is to be feared, it is only to be understood. Now is the time to understand more, so that we may fear less.” -Marie Curie

Perhaps, in the end, it is not about the book you are holding in your hands but more of the people who were involved in the journey - and the path itself. A way to understand more. There are so many people who were involved with this project, who guided me and who shed light on my path during this walk. I can only express my humble gratitude for all of you and I do hope that some day I can give back at least a small part of the light that was given to me during this project. But that is why we are here I guess - to understand and to share what we have learned.

Among the many people involved, I would like to express my gratitude to Timo Kilpeläinen and Peter Sorjonen-Ward for acting as my supervisors and for being there when I needed help. For my co-authors Giulio Viola, Asko Käpyaho, Eveliina Tammisto, Horst Zwingmann, Alexandre Kounov and Marco Andreoli - this is as much yours as it is mine - thank you for everything. Giulio is especially thanked for acting as my mentor during the project and sharing his temper when needed. Grazie mille! This project was initiated during my time at the Geological Survey of Finland and I would like to express my gratitude to Kirsti Loukola-Ruskeeniemi, who provided time, resources and support to start this work. That was the beginning. I then continued with the project at Posiva Oy, which is thanked for supporting the continuation of the work and providing means to an end. Sincere thanks for Ismo Aaltonen and my colleagues at Posiva for all the help and friendship they gave me during this work. It is such a joy to work with all of you! Kerstin Saalman and Mikael Rinne are thanked for their critical review of this thesis.

But most of all, I would like to thank my loved ones - my children Emilia, Onni and Eino and my wife Tara - this thesis is dedicated to you. You are all that I need, thank you for being here with me.

References

- Amantov, A., Laitakari, I., Poroshin, Y. 1996. Jotnian and Postjotnian: sandstones and diabases in the surroundings of the Gulf of Finland. In: Koistinen, T. J. (ed.) Explanation to the map of Precambrian basement of the Gulf of Finland and surrounding area 1 : 1000000. Espoo: Geological Survey of Finland. Special Paper 21, 99-113.
- Anderson, E.M., 1905. The Dynamics of Faulting. Transactions of the Edinburgh Geological Society 8, 387-402.
- Angelier, J., 1994. Fault slip analysis and paleostress reconstruction. In: P.L. Hancock (ed.) Continental Deformation, Pergamon, Oxford, 101-120.
- Angelier, J., 1990. Inversion of field data in fault tectonics to obtain the regional stress — III. A new rapid direct inversion method by analytical means. Geophysical Journal International 103 (2), 363-376.
- Angelier, J., 1984. Tectonic analysis of fault-slip data sets. Journal of Geophysical Research 89 (B7), 5835-5848.
- Angelier, J., 1979. Determination of the mean principal directions of stresses for a given fault population. Tectonophysics 56, T17-T26.
- Angelier, J. & Mechler, P., 1977. Sur une méthode graphique de recherche des contraintes principales également utilisable en tectonique et en seismologie: la méthode des dièdres droits. Bulletin de la Société Géologique de France, 7(19), 1309-1318.
- Barton, C.A., Hickman, S.H., Morin, R., Zoback, M.D., and Benoit, D., 1998. Reservoir- scale fracture permeability in the Dixie Valley, Nevada, geothermal field: Society of Petroleum Engineers Annual Meeting, Trondheim, Abstracts Volume, paper 47371, 315-322.
- Barton, C.A., Zoback, M.D., Moos, D., 1995. Fluid flow along potentially active faults in crystalline rock. Geology, v. 23, p. 683-686
- Bingen, B., Nordgulen, O., Viola, G., 2008. A four-phase model for the Sveconorwegian orogeny, southwestern Scandinavia. Norwegian Journal of Geology 88, 43-72.
- Blenkinsop, T. G. 2006. Kinematic and dynamic fault slip analyses: implications from the surface rupture of the 1999 Chi-Chi, Taiwan, earthquake. Journal of Structural Geology 28, 1040-1050.
- Bott, M.H.P., 1959. The mechanics of oblique slip faulting. Geological Magazine 96 (02), 109-117.
- Byerlee, J., 1978. Friction of rocks. Pure and Applied Geophysics, v. 116, p. 615-626.
- Carey, E., 1976. Analyse numérique d'un modèle mécanique élémentaire appliqué à l'étude d'une population de failles: calcul d'un tenseur moyen des contraintes à partir des stries de glissement. Ph.D. thesis, Univ. Paris-Sud. 138 p.

- Célérier, B., 1995. Tectonic regime and slip orientation of reactivated faults, *Geophysical Journal International*, 121:1, 143-191.
- Collettini, C. & Trippetta, F., 2007. A slip tendency analysis to test mechanical and structural control on aftershock rupture planes. *Earth and Planetary Science Letters* 255, 402–413.
- Delvaux, D., Sperner, B., 2003. New aspects of tectonic stress inversion with reference to the TENSOR program. Geological Society, London, Special Publications 212, 75-100.
- Earnest, E. & Boutt, D., 2014. Investigating the role of hydromechanical coupling on flow and transport in shallow fractured-rock aquifers. *Hydrogeology Journal*, Volume 22, Issue 7, 1573-1591.
- Ehlers, C., Lindroos, A., Selonen, O., 1993. The late Svecofennian granite-migmatite zone of southern Finland – a belt of transpressive deformation and granite emplacement. *Precambrian Research* 64, 295–309.
- Elminen, T., Airo, M.-L., Niemelä, R. Pajunen, M., Wasenius, P., Wennerström, M., 2006. Extensional brittle structures and their relations to the bimodal 1.6 Ga magmatism in the Helsinki region, southern Finland. The 27th Nordic Geological Winter Meeting Abstracts, Bulletin of the Geological Society of Finland, Special Issue I, 31.
- Elminen, T., Airo, M.-L., Niemelä, R., Pajunen, M., Vaarma, M., Wasenius, M., Wennerström, M., 2008. Fault structures in the Helsinki area, Southern Finland. Geological Survey of Finland, Special Paper 47. 185-213.
- Elming, S.-Å., Mikhailova, N. P., Kravchenko, S. 2001. Paleomagnetism of Proterozoic rocks from the Ukrainian shield: new tectonic reconstructions of the Ukrainian and Fennoscandian Shields. *Tectonophysics* 339, 19-38.
- Etchecopar, A., Vasseur, G., Daignieres, M., 1981. An inverse problem in microtectonics for the determination of stress tensors from fault striation analysis. *Journal of Structural Geology* 3, 51-65.
- Ferrill, D.A., Winterle, J., Wittmeyer, G., Sims, D., Colton, S., Armstrong, A., and Morris, A.P., 1999. Stressed rock strains groundwater at Yucca Mountain, Nevada. *GSA Today*, v. 9, no. 5, p. 1–8.
- Fossen, H., 2010. *Structural Geology*. Cambridge, 463 pages.
- Harrison, J.P, Hudson, J.A, Carter, J. N., 2007. Is there a relation between the in situ principal stress magnitudes in rock masses? Proceedings of the 1st Canada-US Rock Mechanics Symposium, Vancouver, Canada, 27–31 May 2007, 675–682.
- Heeremans, M. & Wijbrans, J., 1999. Late Proterozoic tectonic events in Southern Finland, constrained by Ar40/Ar39 incremental heating and single spot fusion experiments on K-Feldspars. *Terra Nova* 11, 216-222.

- Heffer, K.J., & Lean, J., 1993. Earth stress orientation— A control on, and a guide to, flooding directionality in a majority of reservoirs. In: Linville, W., (ed.). Reservoir characterization III: Tulsa, Oklahoma, PennWell Books, 799–822.
- Hickman, S.H., Barton, C.A., Zoback, M.D., Morin, R., Sass, J., Benoit, R., 1997. In situ stress and fracture permeability along the Stillwater fault zone, Dixie Valley, Nevada. *International Journal of Rock Mechanics and Mining Sciences & Geomechanics Abstracts*, v. 34, p. 414.
- Hippolyte, J.-C., Bergerat, F., Gordon, M. B., Bellier, O., Espurt, N., 2012. Keys and pitfalls in mesoscale fault analysis and paleostress reconstructions, the use of Angelier's methods. *Tectonophysics* 581, 144–162.
- Ito, T., & Zoback, M.D., 2000. Fracture permeability and in situ stress to 7 km depth in the KTB scientific drillhole. *Geophysical Research Letters*, Volume 27, Issue 7, 1045–1048.
- Jaeger, J.C., Cook, N.G.W., and Zimmerman, R.W., 2007. *Fundamentals of rock mechanics* (4th edition). Oxford, Blackwell Publishing, 488 p.
- Johansson, E. & Siren, T., 2014. Results of monitoring at Olkiluoto in 2012 - Rock Mechanics. Posiva Report WR 2013-47. Posiva Oy, Eurajoki, 72 p.
- Kohonen, J., Pihlaja, P., 1993. Sedimentation of the Jotnian Satakunta sandstone, western Finland. *Bulletin of the Geological Survey of Finland* 369, 35 p.
- Korja, A., Heikkinen, P., Aaro, S., 2001. Crustal structure of the northern Baltic Sea palaeorift. *Tectonophysics* 331, 341-358.
- Lacombe, O., 2012. Do fault slip data inversions actually yield 'paleostresses' that can be compared with contemporary stresses? A critical discussion. *Comptes Rendus Geoscience* 344, 159-173.
- Lacombe, O., Jolivet, L., Le Pourhiet, L., Lecomte, E., Mehl, C., 2013. Initiation, geometry and mechanics of brittle faulting in exhuming metamorphic rocks: insights from the northern Cycladic islands (Aegean, Greece). *Bulletin de la Société Géologique de France* 184 (4-5), 383-403.
- Lahtinen, R., Korja, A., Nironen, M., 2005. Paleoproterozoic tectonic evolution. In: Lehtinen, M., Nurmi, P.A., Rämö, O.T. (Eds.), *Precambrian Geology of Finland: Key to the Evolution of the Fennoscandian Shield*, *Developments in Precambrian Geology*, vol. 14, pp. 481- 531.
- Lin, A., 2011. Seismic slip recorded by fluidized ultracataclastic veins formed in a coseismic shear zone during the 2008 MW 7.9 Wenchuan earthquake. *Geology* 39, 547–550.
- Lisle, R. J. & Srivastava, D. C., 2004. Test of the frictional reactivation theory for faults and validity of fault-slip analysis. *Geology* v. 32, 569-572.
- Lisle, R.J., 1988. ROMSA: a basic program for paleostress analysis using fault-striation data. *Computers & Geosciences* 14 (2), 255–259.

- Marret, R. & Allmendinger, R. W., 1990. Kinematic analysis of fault-slip data. *Journal of Structural Geology*, Volume 12, No. 8, 973-986.
- Marrett, R. & Peacock, D.C.P., 1999. Strain and stress. *Journal of Structural Geology* 21, 1057-1063.
- McGarr, A. & Gay, N., 1978. State of stress in earth's crust. *Annual Review of Earth and Planetary Sciences* 6, 405-436.
- Mertanen, S., Pajunen, M., Elminen, T., 2001. Applying paleomagnetic method for dating young geological events. *Geological Survey of Finland, Special Paper* 31, 123-129.
- Morris, A. P. & Ferrill, D. A., 2009. The importance of the effective intermediate principal stress (σ_2) to fault slip patterns. *Journal of Structural Geology* 31, 950-959.
- Morris, A.P., Ferrill, D.A., and Henderson, D.B., 1996. Slip tendency analysis and fault reactivation. *Geology*, v. 24, p. 275-278.
- Munier, R. & Talbot, C.J., 1993. Segmentation, fragmentation and jostling of cratonic basement in and near Äspö, southeast Sweden. *Tectonics* 12, 713-727.
- Orife, T. & Lisle, R.J., 2006. Assessing the statistical significance of palaeostress estimates: simulations using random fault-slips. *Journal of Structural Geology* 28 (6), 952-956.
- Pajunen, M. & Wennerström, M., 2010. Development of Brittle Structures in the Satakunta Sandstone (in Finnish). *Geological Survey of Finland, Report of Investigation* 183, 11-63.
- Ploegsma M., 1991. a pilot Rb-Sr dating of the Suomusjärvi ultramylonite: evidence for major Post-Svecofennian deformation in SW Finland. *Bulletin of the Geological Society of Finland* 63, 3-13.
- Pollard, D.D., 2000. Strain and stress: discussion. *Journal of Structural Geology* 22, 1359-1367.
- Posiva 2011. Olkiluoto Site Description 2011. Posiva Report 2011-02. Posiva Oy, Eurajoki, 1030 p.
- Ramsay, J. G. & Lisle, R. J., 2000. *Modern Structural Geology Volume 3: Applications of continuum mechanics in structural geology*. Academic Press.
- Reches, Z., 1978. Analysis of faulting in three dimensional strain field, *Tectonophysics*, 47, 109-129.
- Rämö, O.T. & Haapala, I., 2005. Rapakivi granites. In: Lehtinen, M., Nurmi, P., Rämö, T. (Eds.), *Precambrian Geology of Finland - Key to the Evolution of the Fennoscandian Shield*. *Developments in Precambrian Geology*, vol. 14, pp. 533-562.
- Rogers, S.F., 2003. Critical stress-related permeability in fractured rocks. *The Geological Society of London Special Publication* 209, p. 7-16.

- Rowe, C. D., Kirkpatrick, J. D., Brodsky, E. E., 2012. Fault rock injections record paleo-earthquakes. *Earth and Planetary Science Letters* 335–336, 154–166.
- Rowe, C.D., Moore, J.C., Meneghini, F., McKiernan, A.W., 2005. Large-scale pseudotachylytes and fluidized cataclasites from an ancient subduction thrust fault. *Geology* v. 33, no. 12, 937-940.
- Saalmann, K., Mänttari, I., Ruffet, G., Whitehouse, M. J., 2009. Age and tectonic framework of structurally controlled Palaeoproterozoic gold mineralization in the Häme belt of southern Finland. *Precambrian Research* 174(1-2), 53-77.
- Saalmann, K., 2007. Structural control on gold mineralization in the Satulinmäki and Riukka prospects, Häme Schist Belt, southern Finland. *Bulletin of the Geological Society of Finland*, Volume 79, 69–93.
- Saari, J., 2013. Seismic activity parameters of the Olkiluoto site. Posiva Report 2012-34, Posiva Oy, Eurajoki, 60 p.
- Saintot, A., Stephens, M.B., Viola, G., Nordgulen, Ø., 2011. Brittle tectonic evolution and paleostress field reconstruction in the southwestern part of the Fennoscandian Shield, Forsmark, Sweden. *Tectonics* 30, TC4002.
- Sibson, R. H., 1994. Crustal stress, faulting and fluid flow. Geological Society, London, Special Publications 78, 69-84.
- Suominen, V., 1991. The chronostratigraphy of southwestern Finland: with special reference to Postjotnian and Subjotnian diabbases. *Bulletin of the Geological Survey of Finland* 356, 100 p.
- Torvela, T. & Ehlers, C., 2010. From ductile to brittle deformation - the structural development of and strain distribution along a crustal-scale shear zone in SW Finland. *Int. J. Earth Sci.* 99, 1133 - 1152.
- Torvela, T., Mänttari, I., Hermansson, T., 2008. Timing of deformation phases within the South Finland shear zone, SW Finland. *Precambrian Research* 160, 277-298.
- Townend, J. & Zoback, M., 2000. How faulting keeps the crust strong. *Geology* 28, 399-402.
- Turner, F. J., 1953. Nature and dynamic interpretation of deformation lamellae in calcite of three marbles. *American Journal of Sciences* 251(4), 276–298.
- Twiss, R.J. & Unruh, J.R., 1998. Analysis of fault slip inversions: do they constrain stress or strain rate? *Journal of Geophysical Research* 103, 12205-12222.
- Ujiié, K., Yamaguchi, A., Kimura, G., Toh, S., 2007. Fluidization of granular material in a subduction thrust at seismogenic depths. *Earth and Planetary Science Letters* 259, 307–318.
- Veräjämäki, A. 1998. Pre-Quaternary rocks of the Kokemäki map-sheet area (in Finnish with an English summary). Geological maps of Finland 1:100 000. Explanation to the maps of Pre-Quaternary rocks. Sheet 1134. Espoo: Geological Survey of Finland, 51 p.

Viola, G., Henderson, I.H.C., Bingen, B., Hendriks, B.W.H., 2011. The Grenvillian- Sveconorwegian orogeny in Fennoscandia: back thrusting and extensional shearing along the "Mylonite Zone". *Precambrian Research* 189, 368-388.

Viola, G., Venvik Ganerød, G., Wahlgren, C.-H., 2009. Unravelling 1.5 Gyr of brittle deformation history in the Laxemar-Simpevarp area, SE Sweden: a contribution to the Swedish site investigation study for the disposal of highly radioactive nuclear waste. *Tectonics* 28. TC5007.

Vorma, A. & Niemelä, R. 1994. Geological map of Finland 1:100 000: Pre-Quaternary rocks, sheet 1133 Yläne. Espoo: Geological Survey of Finland.

Väisänen, M. & Skyttä, P., 2007. Late Svecofennian shear zones in southwestern Finland. *GFF*, Volume 129, 55-64.

Wallace, R.E., 1951. Geometry of shearing stress and relation to faulting. *The Journal of Geology* 59, 118-130.

Yamaji, A., 2000. The multiple inverse method: a new technique to separate stresses from heterogeneous fault-slip data. *Journal of Structural Geology* 22, 441-452.